www.czasopisma.pan.pl PAN www.journals.pan.pl
POLSKA AKADEMIA NAUK

Opto-Electronics Review 26 (2018) 279–284

Contents lists available at ScienceDirect

Opto-Electronics Review

journal homepage: http://www.journals.elsevier.com/opto-electronics review

Type-II superlattice detectors for free space optics applications and higher operating temperature conditions

K. Hackiewicz [a,*], P. Martyniuk [a], J. Rutkowski [a], T. Manyk [a], J. Mikołajczyk [b]

[a] Institute of Applied Physics, Military University of Technology, 2 Gen. Witolda Urbanowicza St., 00-908 Warsaw, Poland
[b] Institute of Optoelectronics, Military University of Technology, 2 Gen. Witolda Urbanowicza St., 00-908 Warsaw, Poland

ARTICLE INFO

Article history:
Received 5 July 2018
Accepted 8 August 2018
Available online 14 September 2018

Keywords:
T2SLs
InAs/GaSb
InAs/InAsSb
FSO

ABSTRACT

The utmost limit performance of interband cascade detectors optimized for the longwave range of infrared radiation is investigated in this work. Currently, materials from the III–V group are characterized by short carrier lifetimes limited by Shockley-Read-Hall generation and recombination processes. The maximum carrier lifetime values reported at 77 K for the type-II superlattices InAs/GaSb and InAs/InAsSb in a longwave range correspond to ~200 and ~400 ns. We estimated theoretical detectivity of interband cascade detectors assuming above carrier lifetimes and a value of ~1–50 μs reported for a well-known HgCdTe material. It has been shown that for room temperature the limit value of detctivity is of $\sim 3–4\times 10^{10}$ $cmHz^{1/2}/W$ for the optimized detector operating at the wavelength range ~10 μm could be reached.

© 2018 Association of Polish Electrical Engineers (SEP). Published by Elsevier B.V. All rights reserved.

1. Introduction

A whole range of solutions have been proposed to reach high operating temperature (HOT) conditions of infrared detectors (T > 200 K). The first step is to choose the active region characterized by a high value of the absorption coefficient ratio and thermal generation rate [1]. Among potential materials, in addition to the well-known HgCdTe, should be mentioned type-II superlattices (T2SLs) InAs/GaSb and InAs/InAsSb [2]. Numerical simulations of T2SLs theoretically indicate their better performance compared to HgCdTe. On the other hand, the T2SL InAs/GaSb is characterized by short carrier lifetimes associated with Shockley-Read-Hall (SRH) generation recombination (GR) processes. An improvement in this respect can be reached for T2SLs InAs/InAsSb ("Ga-free" T2SLs) where lack of Ga contributes to the higher carrier lifetimes [3,4].

Another way to increase the operating temperature is a detector's architecture. Structures using non-equilibrium phenomena (exclusion and extraction of carriers from active layer) with suppression of Auger GR process should be distinguished [5]. That approach is commonly used in multilayer HgCdTe structures where carrier concentration is reduced below intrinsic carrier concentration level. In addition to non-equilibrium structures, barrier structures are successfully used to eliminate the SRH component from the depletion area of the barrier absorber heterojunction [6]. The simple architectures of nBn requiring bias (turn on voltage) to operate are commonly used. If application requires zero bias operation pBn barrier detectors must be implemented. Detectors with a unipolar barrier allow to improve detectivity performance close to crossover temperature. A further increase in the operating temperature is possible through the use of a complementary barrier infrared detectors (CBIRD) [7].

The greatest hopes are currently associated with cascade interband detectors (IB CID) that can operate at higher than room temperatures and additionally, in the longwave infrared radiation (LWIR) range, which can be possibly used in free space optics (FSO) applications [8,9].

In the LWIR (λ~10 μm) range a lower influence of absorption and scattering effects are observed. Moreover, there is a lower impact of atmospheric turbulence, as well as less influence of solar radiation compared to commonly used FSO at wavelength of ~1.55 μm. However, the most important advantage is the availability of cascade lasers optimized for this wavelength range. Currently, HgCdTe detectors, which are temperature unstable and T > 300 K operation is difficult to reach, are widely used for FSO - that problem is not the case with structures based on III-V materials [10].

2. Superlattices as a material for HOT detectors

Currently, among materials for HOT detectors, in addition to the well-known HgCdTe, the materials from the 6.1 Å group are used

* Corresponding author.
E-mail address: klaudia.hackiewicz@wat.edu.pl (K. Hackiewicz).

https://doi.org/10.1016/j.opelre.2018.08.001
1230-3402/© 2018 Association of Polish Electrical Engineers (SEP). Published by Elsevier B.V. All rights reserved.

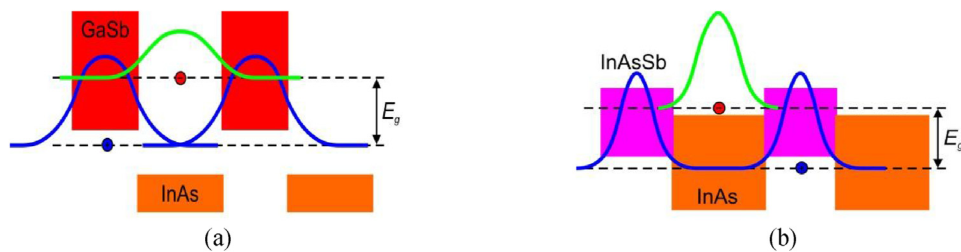

Fig. 1. The wave-function overlapping in a T2SL (a) InAs/GaSb and (b) InAs/InAsSb.

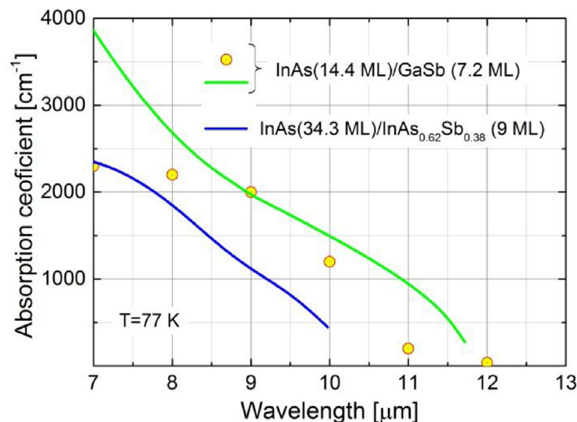

Fig. 2. Simulated and measured absorption coefficient for LWIR T2SLs InAs (14.4 ML)/GaSb (7.2 ML) [experimental data after Ref. [11]. and "Ga-free" T2SLs InAs/InAsSb (x_{Sb} = 0.38) at T = 77 K.

successfully, especially T2SLs InAs/GaSb and InAs/InAsSb. It results directly from the possibilities of these new materials related to energy bandgap engineering (the ability to work in a wide range of radiation depending on the thickness of individual T2SLs' component layers and the chemical composition of InAsSb allows the HgCdTe IR range to be easily covered with both analyzed T2SLs) and limitation of Auger GR processes. The suppression of Auger GR processes results from the specific - mutual arrangement of bands for the type-II (or II "b") superlattice causing spatial separation of the carriers (Fig. 1).

The theoretical estimations of material parameters from the T2SLs in comparison to HgCdTe are better. These include the effective electron masses being not directly dependent on the energy bandgap, and in addition for both T2SLs InAs/GaSb and type-II "b" InAs/InAsSb are higher than those for HgCdTe (assuming the same energy bandgap).

Due to the spatial separation of carriers, the absorption coefficients for the type-II and II "b" superlattices are even two times lower than for HgCdTe. The literature indicates that the absorption coefficient for the InAs/GaSb system operating in the LWIR (λ~10 μm) range equals from 1000 to 3000 cm^{-1} while for "Ga-free" T2SLs is lower [11]. Simulated and measured absorption coefficient for both T2SLs InAs (14.4 ML)/GaSb (7.2 ML) and InAs (34.3 ML)/InAs$_{0.62}$Sb$_{0.38}$ (9 ML) are presented in Fig. 2 [11].

Comparison of carrier lifetime for HgCdTe [12,13] and T2SLs InAs/GaSb [14–20] and InAs/InAsSb [21,22] *vs.* doping concentration at T = 77 K is shown in Fig. 3. The carriers lifetimes being detrimental to a device dark current and quantum efficiency for T2SL materials dedicated to the LWIR range are limited mainly by SRH GR processes and are typically less than 200 ns for T2SLs InAs/GaSb and 400 ns for T2SLs InAs/InAsSb as shown in Fig. 3. However, reported minority carrier lifetimes at 77 K are mainly at the level of ~1–40 ns for LWIR. Comparing those lifetimes with 1 μs reported for Hg$_{0.78}$Cd$_{0.22}$Te there is a huge area for improvement.

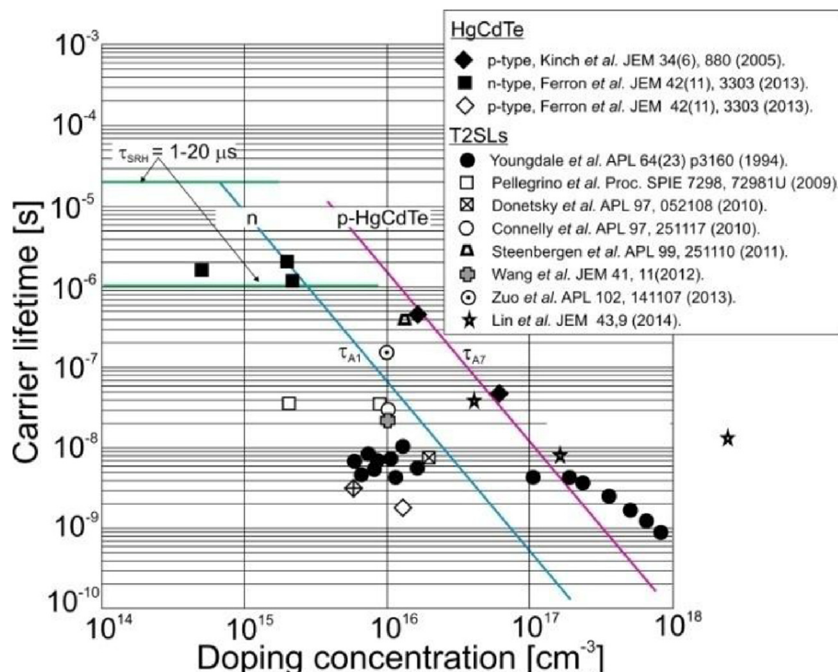

Fig. 3. Carrier lifetimes for LWIR HgCdTe and T2SLs InAs/GaSb, and InAs/InAsSb versus dopping concentration at 77 K.

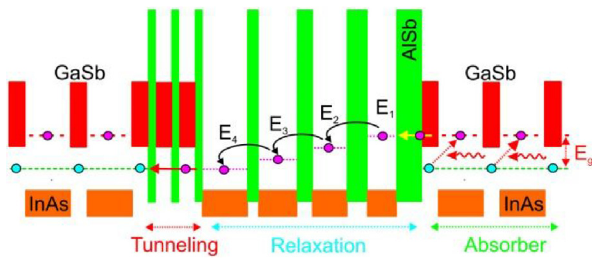

Fig. 4. Schematic illustration of the cascade detector and its components: absorber (T2SL InAs/GaSb), tunneling and transport (relaxation) region.

It is assumed that defects in GaSb layers are responsible for such low carriers lifetime in T2SL InAs/GaSb, therefore the carriers lifetime in type-II "b" superlattice should be higher. Generally, for HgCdTe, the lifetimes are three orders of magnitude higher than those given for materials from group III–V and are placed at the level of 1 μs - 50 ms depending on the material bandgap.

3. HOT cascade detector

The cascade detector consists of several active layers (e.g. InAs/GaSb) with a thickness less than the diffusion length, connected in series by tunneling area (AlSb/GaSb) and the transport (relaxation) area (InAs/GaSb), as exemplified by Fig. 4.

A characteristic feature of the cascade detector is that the photocurrent generated in the structure depends only on the one stage (the last one from the illuminated contact - i.e. the active layer, tunneling layer and transport layer) - and the number of stages directly affects the shot noise, which in turn determines the detectivity according to the dependence:

$$D^* = R_i / \left(\frac{4k_B T}{R_0 A} + \frac{2qJ}{N_S} \right)^{0.5} \tag{1}$$

where: R_i, k_B, T, R_0A, q, J and N_S are the current responsivity, Boltzmann coefficient, temperature, dynamic resistance and detector's area product, elementary electric charge, current density and number of stages, respectively.

Equation (1) indicates that the improvement in detectivity will be visible for the structure being under bias, and the optimal number of stages N_s at which D^* reaches the maximum value (assuming no gain influence) depends on the product of the absorption coefficient $\alpha$and the thickness of the active layer d:

$$N_S = (2\alpha d)^{-1}. \tag{2}$$

4. Limits of performance of cascade detectors optimized on the LWIR range for FSO

In this part the limit performance of cascade detectors based on T2SL InAs/InAsSb operating in the LWIR range will be presented.

In our simulations, a detector based on the T2SLs InAs/GaSb and InAs/InAsSb characterized by a cut-off wavelength $\lambda_{cut\text{-}off}$ = 10 μm (energy bandgap, E_g ~0.124 eV) was used. The dependence on detectivity in case of cascade detectors can be written as (with no gain included):

$$D^* = \frac{\lambda}{hc} \sqrt{N_S} \frac{\eta}{\sqrt{2g_{th} L \tanh(d/L)}} \exp[-\alpha d(N_S - 1)] \tag{3}$$

where: λ, h, c, L, g_{th} and η are the wavelength, Planck's constant, speed of light, diffusion length, thermal generation rate (n_i/τ - the ratio of intrinsic concentration and carrier lifetime) and quantum efficiency [see Eq. (4)], respectively.

$$\eta = \left[\frac{\alpha L}{1-(\alpha L)^2} \right] \times \left[\frac{\sinh(d/L) + \alpha L e^{-\alpha d} - \alpha L \cosh(d/L)}{\cosh(d/L)} \right] \tag{4}$$

The following parameters for superlattice materials (active areas) optimized for LWIR range were assumed in simulations:

- InAs/GaSb - α = 3000 cm^{-1}(maximum value) and τ = 200 ns;
- InAs/InAsSb - α = 2000 cm^{-1}(maximum value) and τ = 400 ns.

The nominal thickness of the active layer, electron and hole mobility were assumed to be 150 nm, μ_e = 0.1 m^2/Vs and μ_h = 0.01 m^2/Vs, respectively.

Fig. 5 shows the detectivity of IB CIDs *vs.* temperature (for a selected number of cascades: N_S = 2, 6, 10, 20, 30) for two T2SLs materials (a) InAs/GaSb and (b) InAs/InAsSb. For temperatures obtained by four-stage thermoelectric (4-TE) coolers (T = 200 K) D^* rates of ~5 × 10^{9}cmHz$^{1/2}$/W for InAs/GaSb and ~1 × 10^{10}cmHz$^{1/2}$/W for InAs/InAsSb were reached. At room temperature, those values are ~2 × 10^9 cmHz$^{1/2}$/W and ~4 × 10^9 cmHz$^{1/2}$/W, respectively. The reported HgCdTe D^* for FSO system operating in LWIR (λ~10 μm) range reaches ~9 × 10^9– 3 × 10^{10} cmHz$^{1/2}$/W at 4-TE–200 K suggesting that T2SLs InAs/InAsSb have potential to meet that requirement. Possible prospect could be estimated above 300 K where assuming growth on GaAs and immersion lens incorporation the D^* could be potentially increased by 10 times.

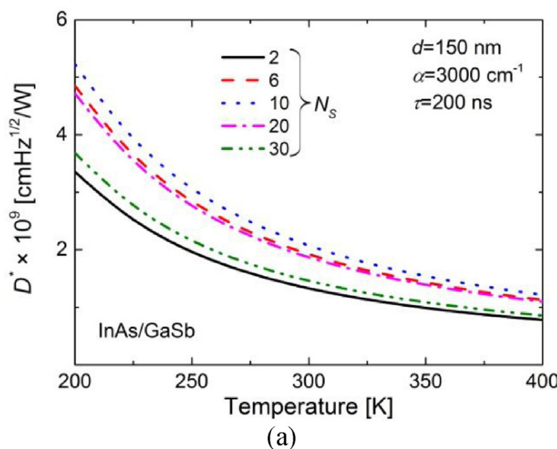

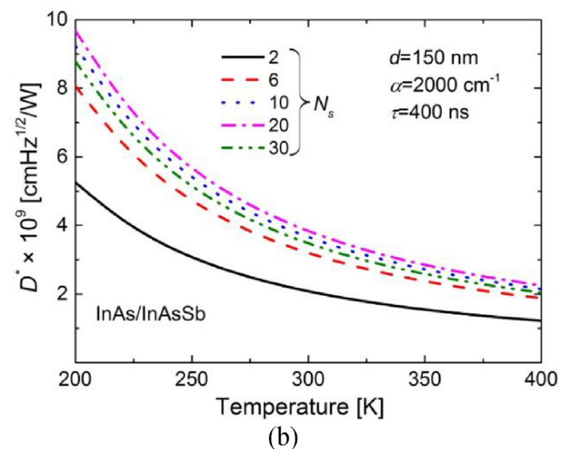

Fig. 5. Limit performance of cascade detectors operating in LWIR regime with active regions: (a) T2SL InAs/GaSb and (b) T2SL InAs/InAsSb, *vs.* temperature for a different number of stages: N_S = 2–30.

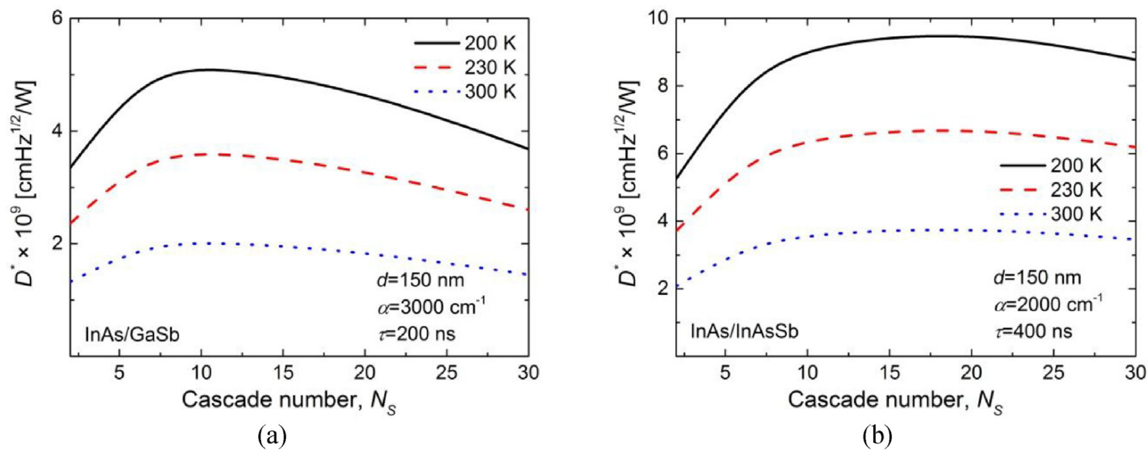

Fig. 6. Limit performance of cascade detectors operating in LWIR regime with active regions: (a) T2SL InAs/GaSb and (b) T2SL InAs/InAsSb, *vs*, number of stages for a selected temperatures: T = 200, 230 and 300 K.

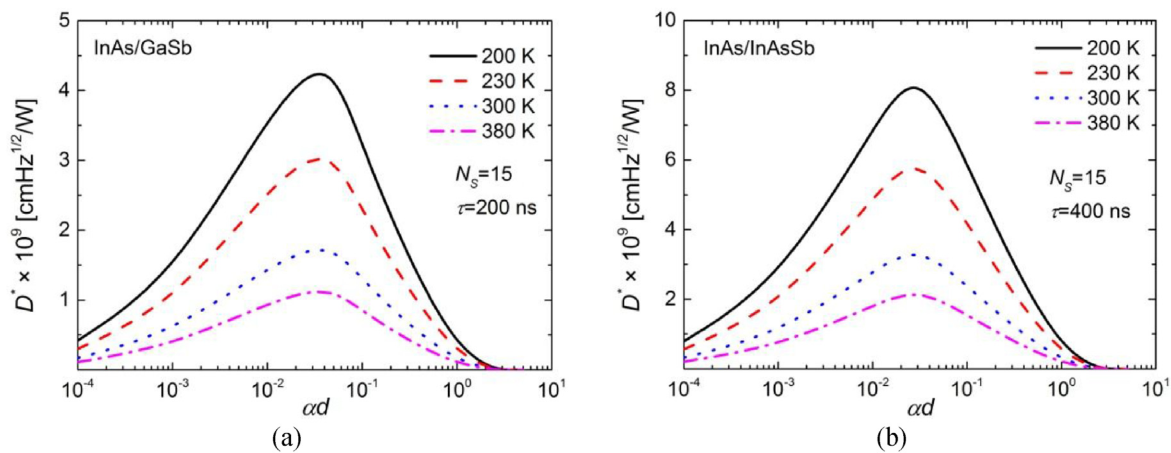

Fig. 7. Limit performance of cascade detectors operating in LWIR regime with active regions: (a) T2SL InAs/GaSb and (b) T2SL InAs/InAsSb, *vs.* αd product for selected temperatures: T = 200, 230, 300 and 380 K.

Figure 6 presents the dependence of limit detectivity *vs*. number of stages. For T2SL InAs/GaSb the highest detectivity is reached for $N_S \sim 10$, while for T2SL InAs/InAsSb for $N_S \sim 17$.

These values correspond directly to the first order approximation which could be extracted from Eq. (3) and is given by Eq. (2). Number of stages for which D^* assumes the highest value depends on reciprocal αd product.

Figure 7 presents utmost D^* simulated *vs*. αd product for selected temperatures T = 200–380 K. Absorber thickness was changed to reach αd within the range of 10^{-4} to 10. Number of stages was assumed 15 for both T2SLs. The optimal αd product increases *vs*. temperature in order to reach maximum D^*.

For T = 300 K and T2SLs InAs/GaSb $\alpha d \sim 0.044$ (where $d \sim$ 146 nm) while for InAs/InAsSb $\alpha d \sim 0.031$ (where $d \sim 155$ nm).

The utmost D^* calculated *vs*. carrier lifetime in the range τ = 10–1000 µs is presented in Fig. 8. Improvement in carrier lifetime by two orders of magnitude leads to D^* increase about ~10 times.

The increase in detectivity can be expected with the improvement of the quality of the material, thus increasing the carrier lifetime. Assuming lifetimes ~50 µs corresponding to the high quality HgCdTe technology, Figure 9 shows the limit values of detectivity. For such assumptions and operating temperature T = 230 K, the $D^* \sim 7 \times 10^{10}$ cmHz$^{1/2}$/W (InAs/InAsSb) can be obtained. For room temperature D^* reaches $\sim 4 \times 10^{10}$ cmHz$^{1/2}$/W.

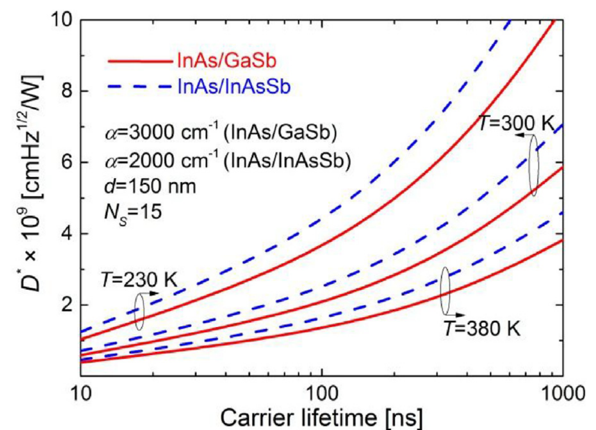

Fig. 8. Limit performance of cascade detectors operating in LWIR regime with active regions: T2SL InAs/GaSb and T2SL InAs/InAsSb, *vs*. carrier lifetime τ = 10 ns – 1 ms for selected temperatures: T = 230, 300 and 380 K.

Comparing that to the background limited D^* (BLIP) calculated for scene temperature, T_S = 300 K and field of view (FOV = 2π) where $D^*_{BLIP} = 5 \times 10^{10}$ cmHz$^{1/2}$/W (for wavelength 10 µm) it could be concluded that there is still area for improvement in terms of both T2SLs carrier lifetimes. The utmost D^* *vs*. wavelength for selected HOT temperatures: 200, 230, 300 and 380 K is presented in Fig. 10.

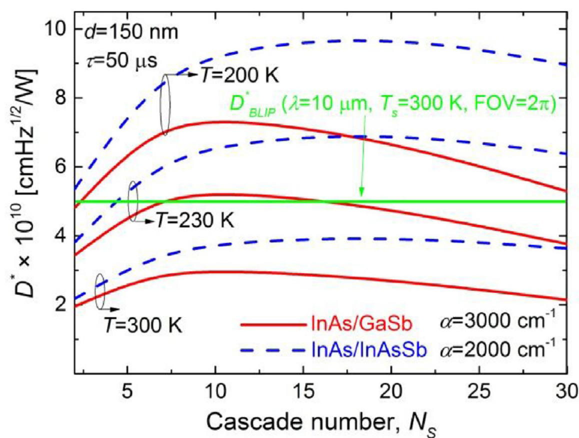

Fig. 9. Limit performance of detectivity *vs.* number of stages for selected temperatures: T = 200, 230 and 300 K, assuming carrier lifetime 50 μs.

The carrier lifetime was assumed at the level of HgCdTe 1 μs for both T2SLs InAs/GaSb and InAs/InAsSb. The simulation results were compared to the D^*_{BLIP} *vs.* λ calculated for scene temperature, T_s = 300 K and FOV = 2π. The simulation results for MWIR and LWIR ranges were compared to the experimental results taken after Tian *et al.* [23], Yang *et al.* [24–26] and Gautam *et al.* [27] for T = 200 and 300 K.

Thermal generation rate at any specific temperature and cut-off wavelength in these devices is usually orders of magnitude smaller than for corresponding intersubband quantum cascade infrared detectors (IC QCIDs). The IC QCID experimental results were presented after Hofstetter *et al.* [28] for T = 100 K. Experimental results presented by Yang *et al.* for LWIR range suggests that carrier lifetime for T2SLs active layers is below assumed 1 μs.

5. Conclusions

For the current state of the technology (carrier lifetime < 400 ns) of T2SLs InAs/GaSb and InAs/InAsSb IB CIDs performance is below HgCdTe used for FSO. However, due to temperature stability, which is difficult to reach for HgCdTe - detectors based on T2SLs can operate above room temperature. In addition, it should be assumed that it will be very difficult to increase the carriers lifetimes limited by the SRH mechanism and that could be circumvented by immersion lens incorporation to increase optical to electrical area ratio.

Acknowledgement

This research was supported by The Polish National Centre for Research and Development grant DOB-BIO8/01/01/2016.

References

[1] A. Rogalski, Infrared Detectors, CRC Press, Boca Raton, 2011.
[2] G.A. Sai-Halasz, L. Esaki, W.A. Harrison, InAs-GaSb superlattice energy structure and its semiconductor-semimetal transition, Phys. Rev. B 18 (6) (1978) 2812.
[3] E.A. Plis, InAs/GaSb type-II superlattice detectors, Adv. Electron. 2014 (2014), 246769.
[4] M. Razeghi, A. Haddadi, A.M. Hoang, G. Chen, S. Bogdanov, S.R. Darvish, F. Callewaert, P.R. Bijjam, R. McClintock, Antimonide-based type II superlattices: a superior candidate for the third generation of infrared imaging systems, J. Electron. Mater. 43 (8) (2014), 28022807.
[5] T. Ashley, C.T. Elliott, Non-equilibrium mode of operation for infrared detection, Electron. Lett. 21 (1985) 451–452.
[6] S. Maimon, G. Wicks, nBn detector, an infrared detector with reduced dark current and higher operating temperature, Appl. Phys. Lett. 89 (2006), 151109.
[7] D.Z. Ting, C.J. Hill, A. Soibel, J. Nguyen, S. Keo, M.C. Lee, J.M. Mumolo, J.K. Liu, S.D. Gunapala, Antimonide-based barrier infrared detectors, Proc. SPIE 7660 (2010), 76601R.
[8] R.T. Hinkey, R.Q. Yang, Theory of multiple-stage interband photovoltaic devices and ultimate performance limit comparison of multiple-stage and single-stage interband infrared detectors, J. Appl. Phys. 114 (10) (2013), 104506.
[9] J. Mikołajczyk, An overview of free space optics with quantum cascade lasers, IJET 60 (3) (2014) 259–264.
[10] J. Mikołajczyk, Z. Bielecki, M. Bugajski, J. Piotrowski, J. Wojtas, W. Gawron, D. Szabra, A. Prokopiuk, Analysis of free-space optics development, Metrol. Meas. Syst. 24 (4) (2017) 653–674.
[11] P.C. Klipstein, Y. Livneh, A. Glozman, S. Grossman, O. Klin, N. Snapi, E. Weiss, Modeling InAs/GaSb and InAs/InAsSb superlattice infrared detectors, J. Electron. Mater. 43 (8) (2014) 2984–2990.
[12] A. Ferron, J. Rothman, O. Gravrand, Modeling of dark current in HgCdTe infrared detectors, J. Electron. Mater. 42 (11) (2013) 3303–3308.
[13] M.A. Kinch, F. Aqariden, D. Chandra, P.-K. Liao, H.F. Schaake, H.D. Shih, Minority carrier lifetime in p-HgCdTe, J. Electron. Mater. 34 (2005) 880–884.
[14] E.R. Youngdale, J.R. Meyer, C.A. Hoffman, F.J. Bartoli, C.H. Grein, P.M. Young, H. Ehrenreich, R.H. Miles, D.H. Chow, Auger lifetime enhancement in InAs-$Ga_{1-x}In_xSb$ superlattices, Appl. Phys. Lett. 64 (1994) 3160–3162.
[15] B.C. Connelly, G.D. Metcalfe, H. Shen, M. Wraback, Direct minority carrier lifetime measurements and recombination mechanisms in long-wave

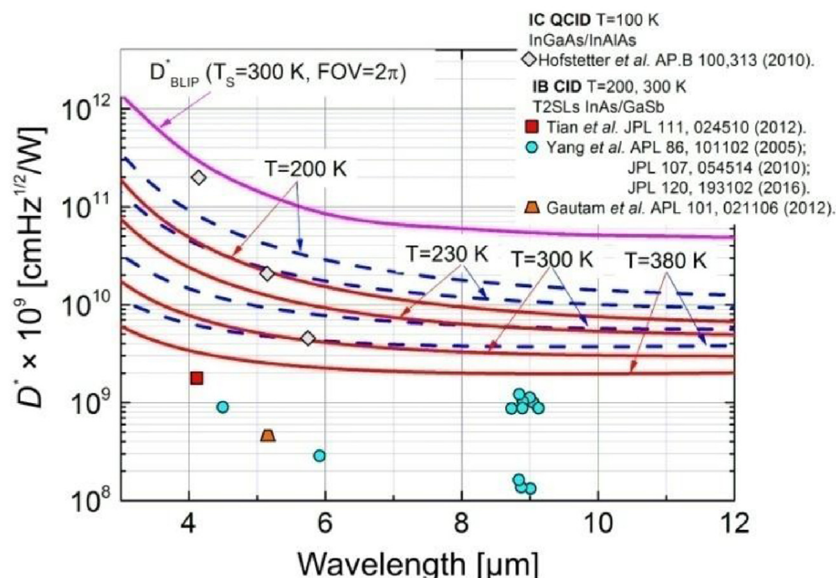

Fig. 10. Limit performance of detectivity *vs.* operating wavelength for selected temperatures: T = 200, 230, 300 and 380 K, assuming carrier lifetime typical for HgCdTe: τ = 1 μs.

infrared type II superlattices using time-resolved photoluminescence, Appl. Phys. Lett. 97 (2010), 251117.
[16] J. Pellegrino, R. DeWames, Minority carrier lifetime characteristics in type II InAs/GaSb LWIR superlattice $n^+\pi p^+$ photodiodes, Proc. SPIE 7298 (2009), 72981U.
[17] D. Donetsky, G. Belenky, S. Svensson, S. Suchalkin, Minority carrier lifetime in type-2 InAs-GaSb strained-layer superlattices and bulk HgCdTe materials, Appl. Phys. Lett. 97 (2010), 052108.
[18] D. Wang, D. Donetsky, S. Jung, G. Belenky, Carrier lifetime measurements in long-wave infrared InAs/GaSb superlattices under low excitation conditions, J. Electron. Mater. 41 (11) (2012) 3027–3030.
[19] D. Zuo, P. Qiao, D. Wasserman, S.L. Chuang, Direct observation of minority carrier lifetime improvement in InAs/GaSb type-II superlattice photodiodes via interfacial layer control, Appl. Phys. Lett. 102 (2013), 141107.
[20] A. Rogalski, M. Kopytko, P. Martyniuk, InAs/GaSb type-II superlattice infrared detectors: three decades of development, Proc. SPIE 10177 (2017), 1017715.
[21] Y. Lin, D. Wang, D. Donetsky, G. Belenky, H. Hier, W.L. Sarney, S.P. Svensson, Minority carrier lifetime in beryllium-doped InAs/InAsSb strained layer superlattices, J. Electron. Mater. 43 (9) (2014) 3184–3190.
[22] E.H. Steenbergen, B.C. Connelly, G.D. Metcalfe, H. Shen, M. Wraback, D. Lubyshev, Y. Qiu, J.M. Fastenau, A.W.K. Liu, S. Elhamri, O.O. Cellek, Y.-H. Zhang, Significantly improved minority carrier lifetime observed in a long-wavelength infrared III–V type-II superlattice comprised of InAs/InAsSb, Appl. Phys. Lett. 99 (25) (2011), 251110.
[23] Z. Tian, R.T. Hinkey, R.Q. Yang, D. Lubyshev, Y. Qiu, J.M. Fastenau, W.K. Liu, M.B. Johnson, Interband cascade infrared photodetectors with enhanced electron barriers and p-type superlattice absorbers, J. Appl. Phys. 111 (2012), 024510.
[24] J.V. Li, R.Q. Yang, C.J. Hill, S.L. Chuang, Interband cascade detectors with room temperature photovoltaic operation, Appl. Phys. Lett. 86 (2005), 101102.
[25] R.Q. Yang, Z. Tian, Z. Cai, J.F. Klem, M.B. Johnson, H.C. Liu, Interband-cascade infrared photodetectors with superlattice absorbers, J. Appl. Phys. 107 (2010), 054514.
[26] N. Gautam, S. Myers, A.V. Barve, B. Klein, E.P. Smith, D.R. Rhiger, L.R. Dawson, S. Krishna, High operating temperature interband cascade midwave infrared detector based on type-II InAs/GaSb strained layer superlattice, Appl. Phys. Lett. 101 (2012), 021106.
[27] L. Lei, L. Li, H. Ye, H. Lotfi, R.Q. Yang, M.B. Johnson, J.A. Massengale, T.D. Mishima, M.B. Santos, Long wavelength interband cascade infrared photodetectors operating at high temperatures, J. Appl. Phys. 120 (2016), 193102.
[28] D. Hofstetter, F.R. Giorgetta, E. Baumann, Q. Yang, C. Manz, K. Köhler, Mid-infrared quantum cascade detectors for applications in spectroscopy and pyrometry, Appl. Phys. B 100 (2010) 313–320.